

Magnetic Weyl Semimetals

Enke Liu[#], Yan Sun, Nitesh Kumar, Aili Sun, Qiunan Xu, Lukas Muehler, Vicky Süß, Claudia Felser

As an edge-cutting topological state, magnetic Weyl semimetals (WSMs) with time-reversal-symmetry breaking are expected to exhibit the fascinating physical behavior of the intrinsic and large anomalous Hall effect (AHE) owing to the nonzero Berry curvature from Weyl nodes, except for the chiral anomaly effect in the bulk and Fermi arc on the surface. In recent years, our group has been searching for magnetic WSMs by combining theoretical calculations, single-crystal growth, and transport measurements. We proposed a novel topological family of Shandite compounds with a Kagomé lattice, in which, for the first time, a magnetic WSM $\text{Co}_3\text{Sn}_2\text{S}_2$ was discovered. While observing the intrinsic anomalous Hall conductivity and giant anomalous Hall angle experimentally simultaneously, we further predicted a high-temperature quantum AHE on the Kagomé lattice with an out-of-plane ferromagnetic order. Our study establishes magnetic Kagomé-lattice WSM as a key material for fundamental research and device applications connecting topological physics and spintronics.

Topological physical states originating from nontrivial band characters have motivated immense interest in the condensed matter physics community. As one of the important exotic states, Weyl fermions stem from the band splitting driven by spin-orbital coupling (SOC) resulting from inversion symmetry breaking or time-reversal-symmetry (TRS) breaking. In magnetic Weyl semimetals (WSMs), two-fold degenerate Weyl fermions are expected to exhibit exotic spin-electronic phenomena. There are currently several proposed magnetic Weyl semimetals. However, few ideal transport experiments on them have been reported. Realization of topological and spintronic transport properties in a magnetic Weyl semimetal is highly desired.

Shandite family with a Kagomé lattice

We recently focused on the Shandite compounds of $\text{M}_3\text{M}'_2\text{X}_2$ (where $\text{M} = \text{Co}, \text{Ni}, \text{Pd}, \text{or Rh}$; $\text{M}' = \text{Sn}, \text{In}, \text{Sb}, \text{Pb}, \text{or Bi}$; and $\text{X} = \text{S}, \text{Se}, \text{or P}$) (Fig. 1a) [1]. The Shandite compounds are an essential family with Kagome lattices. As one Shandite phase, $\text{Co}_3\text{Sn}_2\text{S}_2$ is a ferromagnet with a Curie temperature of 177 K and a magnetic moment = $0.29 \mu_B/\text{Co}$. Band structure calculations revealed that $\text{Co}_3\text{Sn}_2\text{S}_2$ exhibits a half

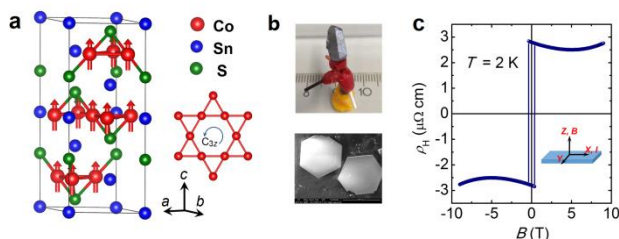


Fig.-1: (a) Unit cell in a hexagonal setting. The Co atoms form a ferromagnetic Kagomé lattice with a C_{3z} rotation. (b) Single crystals grown by different methods. (c) Hall effect at 2 K.

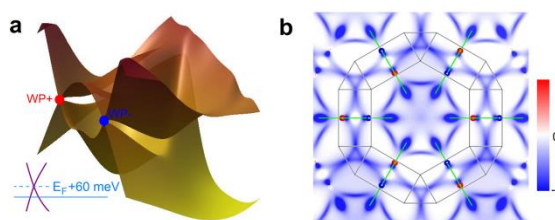


Fig.-2: (a) SOC breaks the nodal ring band structure into opened gaps and Weyl nodes. (b) Berry curvature distribution projected to the k_x - k_y plane.

metallicity in which spin-minority states are gapped. Owing to the extremely strong magnetic anisotropy, the compound shows a quasi-two-dimensional (2D) nature with an out-of-plane magnetization.

Magnetic Weyl phase found by calculations

Our density functional theory (DFT) calculations revealed that there are six nodal rings of linear crossings in the spin-up channel based on band inversion. With SOC the nodal rings were gapped and three pairs of Weyl nodes were formed (Fig. 2a). The Weyl nodes are located 60 meV above the charge neutrality point, which is much closer to the Fermi level than the case for previously proposed magnetic WSMs. The Weyl nodes act as a monopole sink and source of Berry curvature with opposite topological chirality. These Weyl nodes and nontrivial Weyl nodal rings together make this material exhibit a clean topological band structure around the Fermi energy E_F , which further produces enhanced Berry curvature in the Brillouin zone (BZ) (Fig. 2b).

Single-crystal growth

We grew high-quality single crystals by using flux, chemical vapor transport, and Bridgeman methods.

Crystals with sizes from 1 mm to 1 cm can be obtained (Fig. 1b).

Semimetallicity confirmed by the Hall effect

At low temperatures, the magnetoresistance (MR) of the samples is positive and exhibits a non-saturation sign even up to 14 T, which is typical of a semimetal. The nonlinear field dependence of the Hall resistivity (ρ_H) further indicates the coexistence of hole and electron carriers (Fig. 1c), which is in good agreement with our band structure calculations. By using the two-band model, we extract the carrier densities of holes ($n_h \sim 9.3 \times 10^{19} \text{ cm}^{-3}$) and electrons ($n_e \sim 7.5 \times 10^{19} \text{ cm}^{-3}$) of our samples. These relatively low carrier densities and a near compensation of charge carriers confirm the semimetallicity of $\text{Co}_3\text{Sn}_2\text{S}_2$.

Chiral-anomaly-induced negative MR

A Weyl semimetal is expected to exhibit a chiral anomaly in transport measurements, when the conservation of chiral charges is violated in case of a parallel magnetic and electric field. A clear negative MR appears in $\text{Co}_3\text{Sn}_2\text{S}_2$ with a parallel magnetic and electric field. As an equivalent description of the MR, the positive magnetoconductance can be well described by a nearly parabolic field dependence, $\text{MC} \propto B^{1.9}$, up to 14 T (Fig. 3a). In this case, the charge carriers are pumped from one Weyl point to the other one with opposite chirality, which leads to an additional contribution to the conductance, resulting in a negative MR. The chiral anomaly represents an important signature of the Weyl fermions in $\text{Co}_3\text{Sn}_2\text{S}_2$.

Topological surface Fermi arcs

We theoretically studied the surface topological features of $\text{Co}_3\text{Sn}_2\text{S}_2$ (Fig. 3b) [2]. By cleaving the sample at the weak Sn–S bonds, one can achieve two different surfaces terminated with Sn and S atoms, respectively. The resulting Fermi-arc-related states can

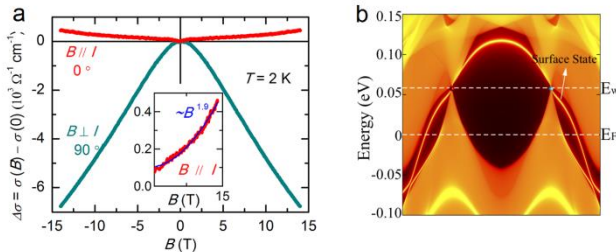


Fig.-3: (a) Magnetoconductance at 2 K in both cases of $B \perp I$ and $B \parallel I$. (b) Energy dispersion for the Sn-terminated surface along a k -path crossing a pair of Weyl points connected by a Fermi arc.

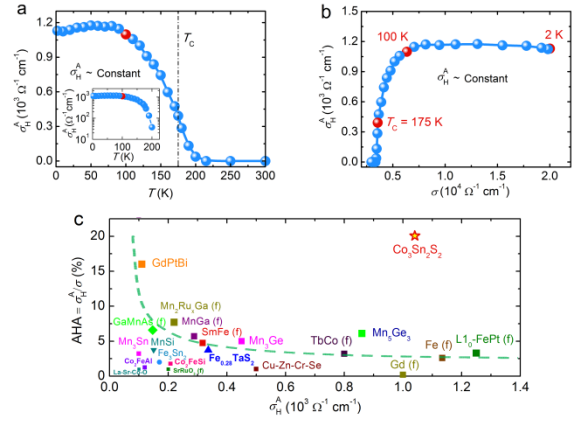


Fig.-4: (a) Temperature dependence of the AHC (σ_H^A) at zero magnetic field. (b) σ dependence of σ_H^A . (c) Comparison of our σ_H^A -dependent AHA results and previously reported data for other AHE materials.

range from the energy of the Weyl points to $E_F - 100$ meV in the Sn-terminated surface. Therefore, it should be possible to observe the Fermi arcs in angle-resolved photoemission spectroscopy (ARPES) measurements. Our ARPES measurements show good agreement of the Fermi surfaces with DFT calculations.

Large, intrinsic anomalous Hall conductivity from Berry curvature

We measured anomalous Hall conductivity (AHC) (σ_H^A) as large as $1130 \text{ } \Omega^{-1} \text{ cm}^{-1}$ at 2 K (Fig. 4a), which is in very good agreement with our predicted theoretical value. Importantly, σ_H^A is revealed to be independent of temperature below 100 K (Fig. 4a). At the same time, σ_H^A is also independent of longitudinal conductivity (σ) below 100 K (Fig. 4b), as is expected for the intrinsic anomalous Hall effect (AHE) in the framework of the unified model of AHE physics. This independence of σ_H^A with respect to both T and σ indicates that the AHE only originates from the intrinsic scattering-independent mechanism and is thus dominated by the Berry curvature in momentum space. By integrating the Berry curvature in the BZ, the AHC (σ_H^A) stays above $1000 \text{ } \Omega^{-1} \text{ cm}^{-1}$ within an energy window of 100 meV below E_F . The DFT calculations are well consistent with our observed scaling behavior, which provides another important piece of evidence for the Weyl phase in $\text{Co}_3\text{Sn}_2\text{S}_2$.

Giant anomalous Hall angle

More importantly, the magnetic Weyl semimetal $\text{Co}_3\text{Sn}_2\text{S}_2$ features a giant anomalous Hall angle (AHA $\sim \sigma_H^A / \sigma$) (Fig. 4c). The temperature dependence of the AHA reaches a maximum of $\sim 20\%$ around 120 K. This is understood by considering that the AHC

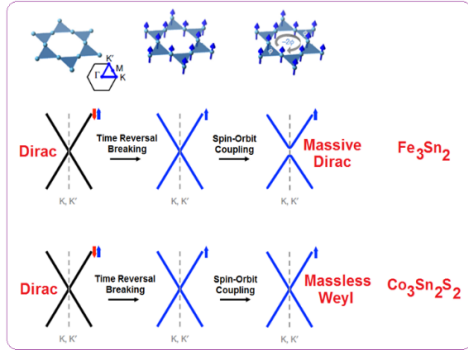


Fig.-5: Comparison of massive Dirac Fe_3Sn_2 and massless Weyl $\text{Co}_3\text{Sn}_2\text{S}_2$. The time-reversal breaking and spin-orbit coupling were applied step by step for clear understanding.

arises from the Berry curvature of the occupied states. The band topology of these states is basically unaffected by the small energy scale of thermal excitations up to room temperature. The topologically protected $\sigma_{\text{H}}^{\text{A}}$ is robust against temperature. In contrast, the Weyl-node-related σ is sensitive to temperature owing to electron–phonon scattering. Therefore, the AHA is expected to increase with increasing temperature in a wide temperature range below T_{C} . The giant AHA comes from the large AHC from enhanced Berry curvature and the low carrier density from semimetallicity.

High-temperature quantum AHE in the 2D limit

The crystal possesses a quasi-2D Co_3Sn layer sandwiched between S atoms, with the magnetic Co atoms arranged on a Kagomé lattice. We investigated the emergence of the quantum AHE in the 2D limit of the magnetic WSM $\text{Co}_3\text{Sn}_2\text{S}_2$ [3]. Two quantum AHE states exist depending on the 2D layer stoichiometry. One is a semimetal with a Chern number of 6, and the other is an insulator with a Chern number of 3. The latter has a band gap of 50 meV, which is much larger than that in magnetically doped topological insulators. Because intrinsic ferromagnets normally have a higher magnetic ordering temperature than dilute magnetic semiconductors, the quantum AHE obtained from this WSM should be stable at higher temperatures.

In summary, we proposed and confirmed $\text{Co}_3\text{Sn}_2\text{S}_2$ as a magnetic WSM. It is the first magnetic WSM that can be characterized by transport measurements, signifying important progress in topological physics. Meanwhile, it is the first material that exhibits intrinsic, strong AHC and giant AHA at the same time owing to significantly enhanced Berry curvature from gapped nodal lines and Weyl nodes. The intrinsic (*not* magnetic doping) out-of-plane ferromagnetic order on

the Kagomé lattice is essential to the promising high-temperature quantum AHE in the 2D limit (i.e., films). The first observation of massless Weyl fermions on a ferromagnetic Kagome lattice provides important progress in studies of the magnetic Kagomé lattice as a well-known quantum model (Fig. 5) [4].

References

- [1] Giant anomalous Hall angle in a half-metallic magnetic Weyl semimetal, E. Liu, Y. Sun, L. Muechler, A. Sun, L. Jiao, J. Kroder, V. Süß, H. Borrmann, W. Wang, W. Schnelle, S. Wirth, S. T. B. Goennenwein, and C. Felser, *arXiv:1712.06722* (2017).
- [2] Topological surface Fermi arcs in magnetic Weyl semimetal $\text{Co}_3\text{Sn}_2\text{S}_2$, Q. Xu, E. Liu, W. Shi, L. Muechler, C. Felser and Y. Sun, *arXiv:1801.00136* (2018).
- [3] Realization of quantum anomalous Hall effect from a magnetic Weyl semimetal, L. Muechler, E. Liu, Q. Xu, C. Felser and Y. Sun, *arXiv:1712.08115* (2017).
- [4] Massive Dirac fermions in a ferromagnetic kagome metal, L. Ye, M. Kang, J. Liu, F. von Cube, C. R. Wicker, T. Suzuki, C. Jozwiak, A. Bostwick, E. Rotenberg, D. C. Bell, L. Fu, R. Comin and J. G. Checkelsky, *Nature* 555 (2018) 638–642.

Enke.Liu@cpfs.mpg.de